Supplementary Material Table of Contents

1. **Supplemental Methods:**

FFPE Sectioned tissue immunofluorescence

Rhesus tissue fixed in house by 4% PFA was processed and embedded in paraffin by the pathology core. 4µm sections of human and rhesus FFPE blocks were performed using the Leica microtome and tissue sections were placed on Superfrost Plus microscope slides. Slides were baked for 15 minutes, followed by deparaffinization in xylene for five minutes with gentle agitation and xylene removed by 100% ETOH wash. Slides were hydrated by 20 dips each in an ethanol dilution series (100%, 70%, 50%, 30%). The slides were washed three times for 5 minutes each in PBS, followed by antigen retrieval with Trilogy (Cell Marque) pretreatment solution for 30 minutes in a rice cooker with boiling water and allowed to cool for one hour. For tissue fixed in formalin for prolonged periods prior to arrival to our center, we performed an additional step of incubating slides in 25% Quadrol at 37ºC for 24 hours after antigen retrieval to reduce autofluorescence. Slides were washed with PBS, three times, 5 minutes each, before and after 25% Quadrol incubation. Following these steps all slides were washed in PBS x 3 times for 5 minutes each. Barriers were drawn around tissue with a hydrophobic pen. The slides were blocked and permeabilized in PBS with 0.3% triton with 10% normal donkey serum for one hour, followed by incubation overnight in primary antibody at 4ºC in humified chamber. Excess antibody was removed by three 5 minutes long washes with PBST. Slides were then incubated in secondary antibody for one hour followed by three washes in PBST for 5 minutes each, protected with Prolong Gold Antifade reagent, and covered.

Thick tissue section clearing and staining

Fresh rhesus kidneys shipped on ice were fixed in 4% paraformaldehyde (PFA) for 48 hours at 4ºC, followed by five washes in PBS for 5 minutes (min) each. Pre- fixed tissue in formalin was washed in PBS five times for 5 min each and stored in PBS with 0.01% sodium azide. Tissue was manually sectioned into cross sectional and cortical 500 micrometer sections using a razor blade

and slicer matrix designed by CCHMC clinical engineering using the Fortus 250 (Stratasys) 3D printer and ABS plus material. Rhinoceros 3d (CAD) software was used to design the cutting mold, and Stratasys Insight software was used to slice the design file and create the G-code to run the printer (code available upon request). Tissue sections were submerged in 25% N,N,N′,N′-Tetrakis(2-Hydroxypropyl)ethylenediamine (Quadrol) and rocked at 37ºC for 24 hours to aid in reducing autofluorescence[1, 2]. Tissue sections were then embedded in 4% acrylamide hydrogel with 0.25% of the photoinitiator 2,2′-azobis[2-(2-imidazolin-2-yl)propane] dihydrochloride (Wako Pure Chemical) for a minimum of 24 hours at 4°C, followed by 3 hours of heating at 37°C for polymerization of the gel as previously described[3]. The tissue was washed five times in PBS at room temperature (RT) for 1 hour each to remove excess hydrogel, then cleared using 8% sodium dodecyl sulfate (SDS) in 0.1M PBS [4] solution and rocked in 37°C for 48-72 hours until clear, with exchanges of SDS every 24 hours. Following clearing, the tissue was washed in milli-Q water for three exchanges (30 min-1 hour) at 37°C, followed by five washes in PBS at RT (30 min-1 hour, including one overnight wash) to remove any excess SDS. Cleared tissue was blocked for 24 hours at RT rocking in 6% bovine serum albumin (BSA), 0.1% triton, 0.01% sodium azide, with 5% normal donkey serum (NDS) followed by incubation in primary antibodies for four days rocking at 37°C (with fresh antibody exchange after 48 hours). The tissue was washed five times in PBS with 0.1% tween (PBST) at room temperature for 1 hour each, as well as one overnight wash at RT, followed by incubation in secondary antibody for four days rocking at 37°C. After washing the tissue in PBST five times at room temperature for 30 min to 1 hour each, as well as one overnight wash at RT, the kidney tissue was incubated in Refractive Index Matching Solution (RIMS)[3] for a minimum of 24 hours at 4°C until tissue appeared clear by visual inspection.

Quantitative image analysis of cleared tissue:

3D tissue z-stack Images were processed using Bitplane Imaris 9.3.1. Surfaces were created using surface rendering using the background subtraction/local contrast setting. To quantify the

average length to the last branch point in rhesus kidneys, the cross-sectional kidney samples were measured from cortex to base to a maximum depth of 850μm to standardize depth analysis for all samples. Surfaces for KRT8 and/or CDH1 were created. Branch point depth in 797 ureteric stalks from 126 to 138 DG in the rhesus and 53 ureteric stalks in the 32-WG human were individually determined by the investigator. Stalks meeting at a bifurcating branch point was counted as a single branch point and discounted from the single stalks count. Distances between last bifurcation point to cortical surface was measured using the measurement tool in Imaris by selecting points on surface from branch point to tip of ureteric stalk.

Niche tips were quantified using “spot detection” of the surfaces rendered ureteric tip using KRT8 and/or CDH1. White spheres indicate individual tip termini, which were measured to analyze tip-to–nearest-tip distances. Matlab extension was used to calculate the nearest nephrogenic tip using “spot to spot closest distance” function from center of each spot. The investigator confirmed that every UB tip was counted once prior to calculation. The number of niche tips per cluster was determined by 3D rendering and confirmed by visually following the ureteric stalk through the 500μm z-stack using elements software.

Single molecule Fluorescent in Situ Hybridization (smFISH) using RNAScope®

RNAScope was performed using the Multiplex Fluorescent V2 Assay (Advanced Cell Diagnostics, Inc (ACD)). Positive controls used were human PPIB (medium abundance) and Pol2RA (low abundance). The negative bacterial control (DapB) was used on all tissue samples. Probes used included Human SIX1, SHISA8, CACNA1E, PTCHD1, ATP1A4, CCL26, TWIST1, POU3F4, AKR1C1, SAMSN1, and GCNT4. When needed, custom probes were designed with the assistance of ACD. 4μm formalin-fixed paraffin-embedded human kidney sections were deparaffinized and dehydrated according to manufacturer’s protocol. This was followed by peroxidase quenching, target retrieval, and protease digestion. Target probes, positive control probe, and negative control probe were incubated on respective slides for 2 hours at 40ºC, followed by amplification per protocol guidelines. The amplified signal was conjugated to Opal

fluorophore (Opal 520, Opal 560, Opal 650; PerkinElmer). Following completion of manufacturer's recommendation for RNAScope V2 kit, slides were blocked at RT for 1 hour in Tris-buffered saline (TBS) with 1% BSA, 5% normal goat serum and incubated in primary antibody guinea pig anti-cytokeratin 8/18 (Abcam) overnight at 4ºC, followed by three washes in TBS with 0.05% tween for five minutes each at RT, and then secondary antibody incubation for 1 hour with goat anti-guinea pig 750 (Millipore). Slides were washed three times in TBS with 0.05% tween for five minutes each at room temperature (RT), and then mounted with prolong gold antifade reagent.

Quantitative analysis of RNAScope

Regions of interest (ROI) measuring 300x300pixels were chosen based on whether the 40x image contained NPC, differentiated NPC, or stroma. To remove any conflated counts by red blood cell interference, any signals with mean intensity signal > 500 in the autofluorescent channel (DAPI) was removed from the total transcript count. NPC was further broken down into NPC 1(closest to cortical surface), NPC 2 (farther from cortical surface) and NPC3 (farthest from cortical surface, see figure 4C for example). Differentiated NPC was chosen by anatomic location below the NPC/tip niche based on krt8 staining. At least three ROIs were analyzed per sample of each NPC region. Cropped 300x300pixel ROI were converted to Imaris files. All display adjustments in Bitplane Imaris 9.3.1 retained the same configuration as initial acquisitions to confirm accurate counts. We used the "spots" algorithm to identify individual transcripts based on an estimated transcript diameter of 0.4µm and the fluorescence detection threshold at 488, TRITC, and Cy5, respectively, based on negative controls for the respective channels. Algorithm settings remained consistent for both negative control slides and all human tissue samples. All negative controls had an average of 3 or less spots per 300x300pixel region (supplemental data 2). To determine the change in SHISA8, we tabulated the absolute transcript counts for the three NPC zones. In the young samples (16-17WG), The median SIX1 transcript count at NPC1 was 100.5 (range 52-134), decreasing to ~80(78 (52-185) and 80.5 (49-127) at NPC2 and 3, respectively). In old samples (26-27WG), the median *SIX1* count at NPC1 was 56 (31-199), increasing to 124 (49-

316) in NPC 2 and 94 (44-94) in NPC3. The median *SHISA8* transcript count at NPC1 and NPC2 in the young samples was ~22 (21.5 (6-51) in NPC1 vs 22 (16-37) in NPC2), increasing to 33 (16-48) in NPC 3. In old samples, the median *SHISA8* transcript count was 15 (5-43) in NPC1, increasing to 41 (11-69) and 55 (11-131) at NPC2 and 3, respectively. The data were expressed as absolute *SHISA8* counts and a *SHISA8/SIX1* ratio.

Single Cell Suspension Preparation, scRNA-seq procedure, and snRNA-seq procedure

For three samples, the cortical region was removed manually with forceps and sterile scalpel and placed in ice-cold PBS in a biosafety hood. All steps in the dissociation, except centrifugation, were carried out on ice in a biosafety hood. Centrifugation steps were carried out at 4 °C for 5 min. The tissue was minced on ice using a razor blade into a fine paste. 40 mg of minced tissue was mixed with 2 mL cold-active enzyme mix (8 mg/mL Collagenase A (Roche 10103586001), 8 mg/mL Coll. Type 4 (Worthington LS004186), 125 U/mL DNase (Applichem A3778), 5 mM $CaCl_2$ made up in DPBS (ThermoFisher 14190)) and split into two tubes that were shaken vigorously 3-5 times every 30 sec. At 2 min, trituration was commenced with 1ml pipette applying 10 strokes every 2 min, with the tip cut, with vigorous shaking every min between strokes. After 20 min, the tissue pieces were allowed to settle on ice for 1min. 750µl of the single cell supernatant was removed and gravity-filtered by a 30 µM sieve (Macs smart Filter, Miltenyi) in 50 mL conical tube on ice. 15 mL ice-cold PBS/BSA 0.04% was used to rinse the 30 µM filter and to dilute the filtrate. The flow-through was kept on ice with the filter. In parallel, 1 mL of enzyme mix (previous mix with 100 µg/mL soybean trypsin inhibitor added (Roche, 10109886001)) was added to 250µl in each of the two original 1.5 ml tubes with settled tissue chunks. The tubes were then triturated every two min with an intact 1ml pipette tip and shaken between strokes for 11 repetitions until tissue clumps were broken down, and the content added to the same 30 µM filter from the previous step. The filter rinsed with 10 mL ice-cold PBS/BSA bringing the total volume to 28.5ml. The combined flow-through from the two rounds was split between two 15 mL conical tubes and spun at 250G. The supernatant was removed, leaving approximately 100 µL in each tube. Cell pellets were re-

suspended in 2 mL of red blood cells (RBC) lysis buffer (Sigma, R7757) total and combined. Cells were triturated again for 20 times and incubated on ice for 4 min. Cells were re-filtered through a 30 μM filter into a 50 mL conical tube, followed by 11 mL of ice-cold PBS/BSA, transferred to a 15ml conical tube and pelleted at 250G. The supernatant was removed, and the RBC lysis step repeated with 3 mL RBC lysis buffer. The cells were filtered as above with a new 30 μM filter followed by 24 mL of ice-cold PBS/BSA. The flow-through was transferred to two 15 mL conical tubes and spun at 200G. The cell pellets were combined in 100 μL total volume PBS/BSA and inspected for the presence of RBC. If RBC are visualized in the re-suspended cells, the steps above were repeated until RBC were no longer visible.

After the last RBC lysis step, the cells were spun and the supernatant was removed; cells were re-suspended in 1 mL ice-cold PBS/BSA, transferred to a 1.5 mL tube and pelleted at 550G in a swinging bucket centrifuge. Supernatant was removed, and the pellet re-suspended in 100 μL ice-cold PBS/BSA. Cell viability and concentration were determined with a hemocytometer using trypan blue. 10,000 cells were loaded into the 10x Genomics controller to target recovery of 6000 cells. Excess dissected cortex was frozen in liquid nitrogen.

For the 130-day kidney scRNA seq sample, all steps in the dissociation, except centrifugation and vortexing, were carried out in a biosafety hood on ice. Kidneys were isolated and the kidney capsule and fatty tissue removed. One whole kidney was placed in a 50 mL conical with 5 mL B. Lich enzyme mix (10 mg/mL B. Lich (Sigma P5380) 0.5 mM EDTA made up in DPBS (ThermoFisher 14190)). The conical was transferred to a cold room on ice and vortexed on setting 3 for 5 min. Supernatant was saved, and additional 5 mL of B. Lich enzyme mix was added to the kidney in the 50 mL conical. The tube was vortexed gently at 4 °C for 4 min. This was repeated for three total rounds. Removed supernatants from each round were immediately filtered using a new 30 μM filter for each round, followed by rinsing the filter with 10 mL ice-cold PBS/BSA 0.04% and transferring the flow-through to a 15 mL conical, and spinning at 500G. Supernatant form each round was discarded, and the pellets re-suspended in 5 mL ice-cold PBS/BSA. The

flowthroughs from all three rounds were combined and spun at 500G for 5 min. Supernatant was removed and the pellet re-suspended in 1 mL ice-cold PBS/BSA. The cell mix was applied to a 20μM filter (PluriSelect) on a 50 mL conical and the filter was rinsed with 10 mL ice-cold PBS/BSA. The flow-through was transferred to a 15 mL conical and spun at 500G. The supernatant was discarded, and the cells were re-suspended in 500 μL ice-cold PBS/BSA. Cell viability and concentration was analyzed using a hemocytometer with trypan blue. 12,300 cells were loaded into the 10x controller, targeting the capture of ~8000 cells. For snRNAseq protocol, the nuclei were isolated from this frozen tissue using a protocol described previously[5] using 30 strokes of the loose pestle and 13 strokes of the tight pestle and a final filtration with a 10 μM filter. The flow through nuclei were suspended in 0.04% BSA/PBS with 40 u/mL RNAse Inhibitor (Promega, N2615)

Single-Cell Analyses

The raw scRNA-Seq and snRNA-Seq data (10x Genomics 3' version 3) were aligned to the Ensembl version 91 reference transcriptome using the Cell Ranger version 3.1.0 workflow. For the snRNA-Seq, a combined intron-exon reference was produced as described using the vendor-provided “Generating a Cell Ranger compatible “pre-mRNA” Reference Package” guidelines (https://support.10xgenomics.com/single-cell-gene-expression/software/pipelines/latest/advanced/references), prior to analysis. From the output for Cell Ranger for the snRNA-Seq, we corrected for ambient background RNA using the R package SoupX, selecting a correction factor of 0.5. In SoupX, we used the inferNonExpressedGenes() function to determine which genes had the highest probability of being ambient mRNA, and the strainCells() function in order to transform count matrices. The unique molecular index (UMI) counts produced from these analyses were scaled per cell (counts per ten-thousand) and log2 adjusted in the software AltAnalyze version 2.1.4 (EnsMart 91, Macaca mulatta database) using the “--dataFormat counts” option. Counts from all biological replicates of the cortex scRNA-Seq (Cell Ranger filtered matrix barcodes) were combined prior to further analysis (--

accessoryAnalysis MergeFiles option). To identify cell populations in both the scRNA-Seq and snRNA-Seq, the software ICGS2 (Iterative Clustering and Guide-gene selection version 2), was run using the default options (cosine clustering) in addition to stringent exclusion of cell-cycle effects(--excludeCellCycle)[6]. Associated UMAP and marker genes (MarkerFinder algorithm) were directly obtained from the ICGS2 results. These same unsupervised single-cell analyses were also applied to previously reported human scRNA-Seq from multiple 16-17-week fetal samples, to identify integrated NPC cell cluster cells (GSE112570, GSE102596). Refined UB clusters were produced from two scRNA-Seq clusters (c11 and c13) were subclustered using this same protocol, following removal of single-cell clusters using the software DoubletDecon. In brief, the 37-cluster ICGS2 scRNA-Seq heatmap supplied as input to DoubletDecon, using default options (default cluster merging option (ρ′)), to identify 2,615 predicted doublets (11% of cells). As these estimates were predicted to overcall doublets, we examined the initial sub-clustering of UB and identified a small population enriched in markers of Proximal tubule, in which >95% of cells were predicted to Proximal/UB doublets. After removing all cells in this doublet cluster (all other doublets were infrequent in ICGS2 UB clusters), the data were re-analyzed with ICGS2. All ICGS2 produced clusters were assigned preliminary names based on GO-Elite gene-set enrichment to the human fetal kidney cell populations Lindstrom et al[7], which were incorporated into a new single-cell marker gene compendium of over 2,300 cell-population signatures from 52 independent human adult and fetal single-cell genomics studies, manually extracted or from the CellMarker database (AltAnalyze version 2.1.4 BioMarker database) (**Table S6**)[8]. In cases where the top-enriched predicted cell type was unrelated to kidney, the highest scoring kidney cell type was assigned or replaced based on a manual literature evaluation of top-ranked ICGS2 marker genes and visualization in the produced interactive web browsers (see Table S7). To project single-cell populations from the scRNA-Seq to the snRNA-Seq, we used the cellHarmony workflow using the ICGS2 marker-gene cluster centroids as the reference for direct alignment, with a Pearson rho cutoff > 0.1[9]. For joint-analysis of the scRNA-Seq, Seurat version 3.1.0 was

run using the integration option with counts data normalized using the “LogNomalize” option as scaled to 10,000 (default). Here, four of the Rhesus scRNA-Seq, the Rhesus snRNA-Seq and the three human 16-17 week scRNA-Seq captures were integrated. Rhesus gene IDs were mapped to their closest orthologues using the Ensembl BioMart database (version 91). The feature selection was performed to identify the top 6000 most variable genes using “vst” option. PCA based dimension reduction using the most variable genes (n=2000). The first 30 dimensions were considered for PCA, UMAP and to find neighbors. Louvain clustering was performed with a resolution cutoff=1.0. The raw scRNA-Seq and snRNA-Seq are deposited in GEO (GSE158304 – reviewer token: gzwfaqygvdkplup) and the aligned and processed data are deposited in Synapse (syn22647742 – username: Reviewer-CCHMC, password: Reviewer-CCHMC1).

Lineage Trajectory Analysis

To infer predicted pseudotime trajectories within the full rhesus scRNA-Seq dataset, we applied the SlingShot software[10] on the ICGS2 obtained UMAP cell-barcode coordinate plot. SlingShot results are displayed as a radial graph with the self-renewing NPCs (cluster 25) as the origin cluster, after manually excluding non-epithelial cell coordinates from the plot. As a secondary means of evaluating lineage trajectories, we applied the Velocyto toolkit, to examine predicted differentiation trajectories by virtue of the RNA velocity of spliced versus unspliced transcripts in the snRNA-Seq data using the SeuratWrappers framework[11]. Predictions from this workflow were projected onto the ICGS2 UMAP embeddings using the CreateDimReducObject() function. To evaluate possible developmental transitions from the sub-clustered UB cells, the scaled/log-transformed expression matrix and cell cluster labels from ICGS2 were provided as the input to Monocle2. The log-transformed file was exponentiated and the expression family parameter (‘expressionFamily’) was set to tobit. Monocle2 was allowed to select its own genes for pseudotime estimation but the differential gene test was run using ICGS2 groups (‘fullModelFormulaStr = ~Groups). The reduction method was set to the default option, PCA, and

the reverse graph embedding (RGE) method ('method' in reduceDimension) was set to "DDRTree".

References:

1. Tainaka K, Shimpei, Takeru, Etsuo, Perrin D, Ukai-Tadenuma M, et al.: Whole-Body Imaging with Single-Cell Resolution by Tissue Decolorization. *Cell,* 159**:** 911-924, 2014 10.1016/j.cell.2014.10.034
2. Jing D, Zhang S, Luo W, Gao X, Men Y, Ma C, et al.: Tissue clearing of both hard and soft tissue organs with the PEGASOS method. *Cell Res,* 28**:** 803-818, 2018 10.1038/s41422-018-0049-z
3. Lee E, Choi J, Jo Y, Kim JY, Jang YJ, Lee HM, et al.: ACT-PRESTO: Rapid and consistent tissue clearing and labeling method for 3-dimensional (3D) imaging. *Sci Rep,* 6**:** 18631, 2016 10.1038/srep18631
4. Yang B, Treweek JB, Kulkarni RP, Deverman BE, Chen CK, Lubeck E, et al.: Single-cell phenotyping within transparent intact tissue through whole-body clearing. *Cell,* 158**:** 945-958, 2014 10.1016/j.cell.2014.07.017
5. Wu H, Kirita Y, Donnelly EL, Humphreys BD: Advantages of Single-Nucleus over Single-Cell RNA Sequencing of Adult Kidney: Rare Cell Types and Novel Cell States Revealed in Fibrosis. *Journal of the American Society of Nephrology,* 30**:** 23-32, 2019 10.1681/asn.2018090912
6. Venkatasubramanian M, Chetal K, Schnell DJ, Atluri G, Salomonis N: Resolving single-cell heterogeneity from hundreds of thousands of cells through sequential hybrid clustering and NMF. *Bioinformatics,* 36**:** 3773-3780, 2020 10.1093/bioinformatics/btaa201
7. Lindstrom NO, Guo J, Kim AD, Tran T, Guo Q, De Sena Brandine G, et al.: Conserved and Divergent Features of Mesenchymal Progenitor Cell Types within the Cortical Nephrogenic Niche of the Human and Mouse Kidney. *J Am Soc Nephrol,* 29**:** 806-824, 2018 10.1681/ASN.2017080890
8. Zhang X, Lan Y, Xu J, Quan F, Zhao E, Deng C, et al.: CellMarker: a manually curated resource of cell markers in human and mouse. *Nucleic Acids Res,* 47**:** D721-d728, 2019 10.1093/nar/gky900
9. DePasquale EAK, Schnell D, Dexheimer P, Ferchen K, Hay S, Chetal K, et al.: cellHarmony: cell-level matching and holistic comparison of single-cell transcriptomes. *Nucleic Acids Res,* 47**:** e138, 2019 10.1093/nar/gkz789
10. Street K, Risso D, Fletcher RB, Das D, Ngai J, Yosef N, et al.: Slingshot: cell lineage and pseudotime inference for single-cell transcriptomics. *BMC Genomics,* 19**:** 477, 2018 10.1186/s12864-018-4772-0
11. La Manno G, Soldatov R, Zeisel A, Braun E, Hochgerner H, Petukhov V, et al.: RNA velocity of single cells. *Nature,* 560**:** 494-498, 2018 10.1038/s41586-018-0414-6

2. Supplemental Figures

Figure S1

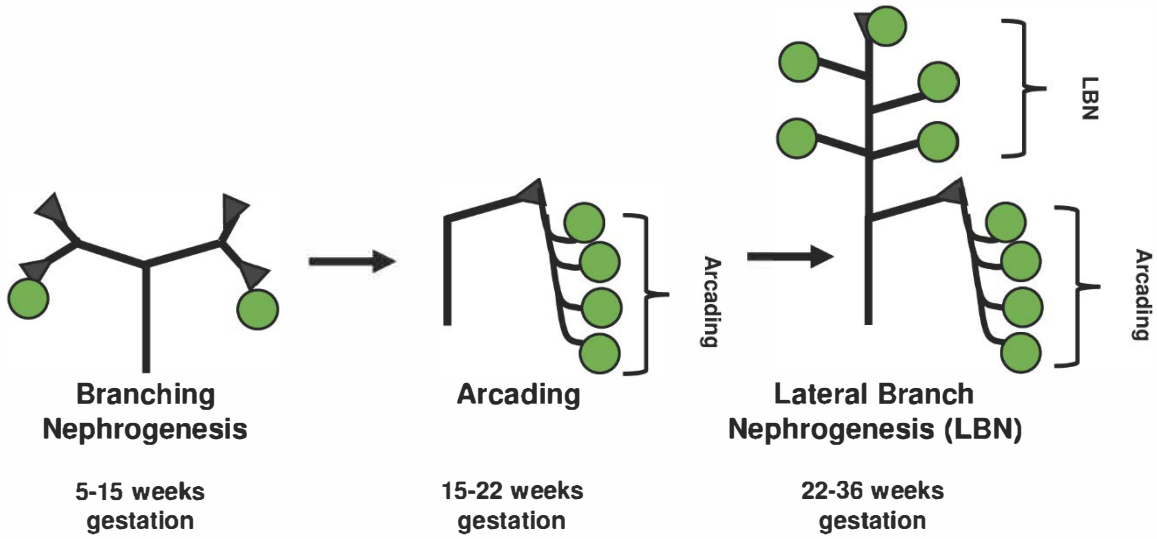
LBN
Arcading
Arcading
Branching Nephrogenesis
5-15 weeks gestation
Arcading
15-22 weeks gestation
Lateral Branch Nephrogenesis (LBN)
22-36 weeks gestation

Figure S2

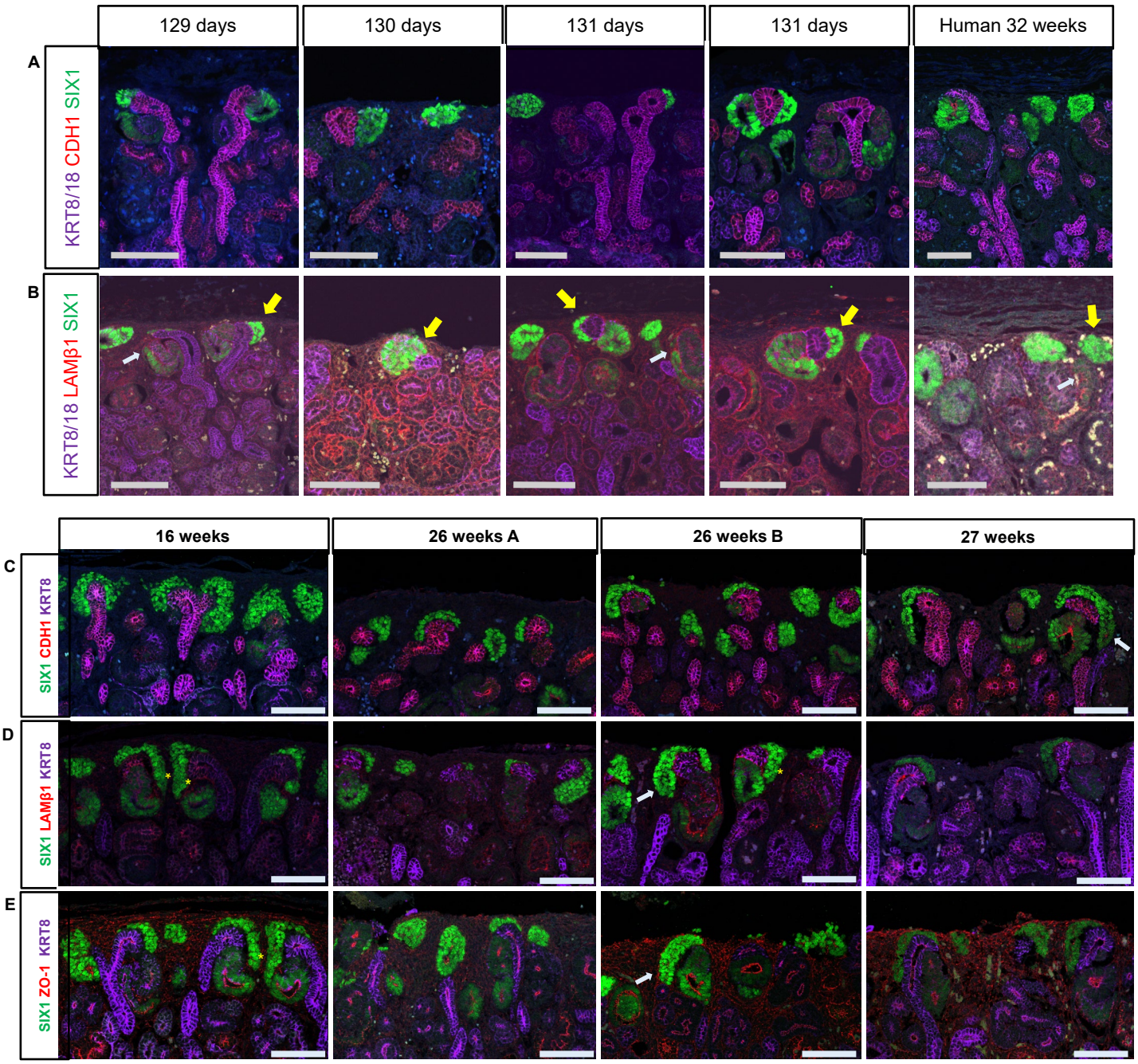
129 days
130 days
131 days
131 days
Human 32 weeks
A
KRT8/18 CDH1 SIX1
B
KRT8/18 LAMβ1 SIX1
16 weeks
26 weeks A
26 weeks B
27 weeks
C
SIX1 CDH1 KRT8
D
SIX1 LAMβ1 KRT8
E
SIX1 ZO-1 KRT8

Figure S3

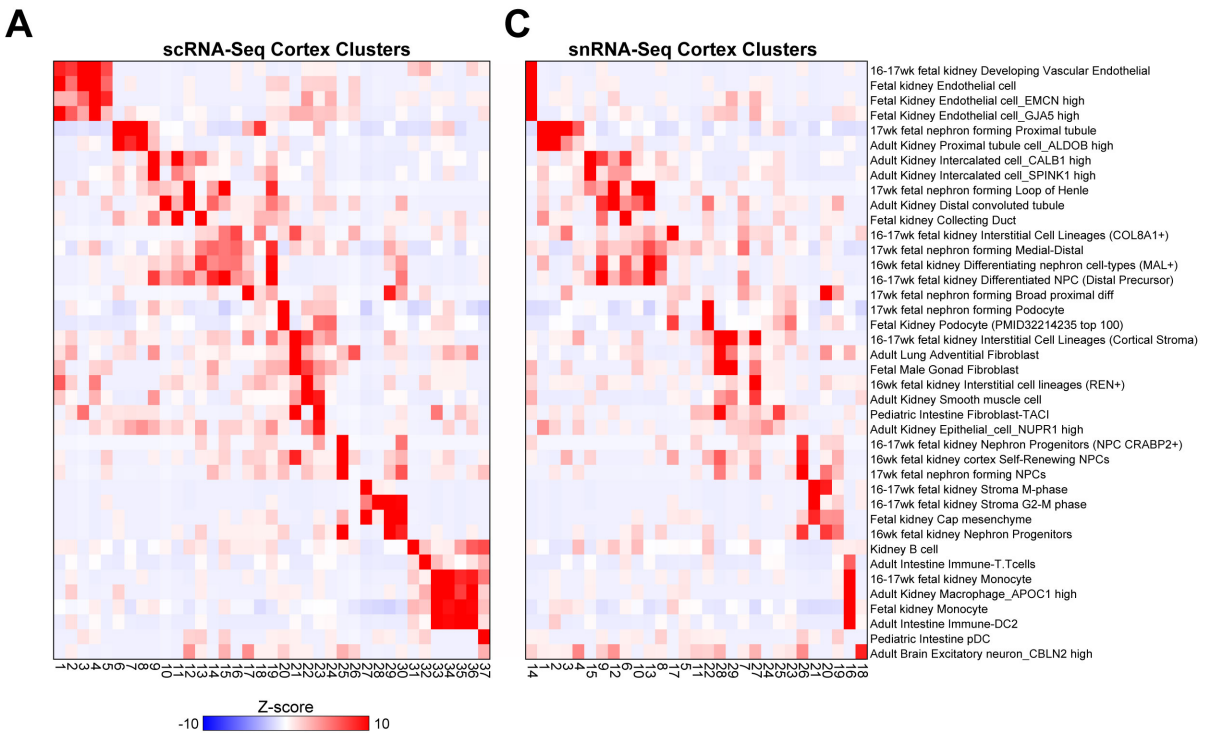
A
scRNA-Seq Cortex Clusters
C
snRNA-Seq Cortex Clusters
16-17wk fetal kidney Developing Vascular Endothelial
Fetal kidney Endothelial cell
Fetal Kidney Endothelial cell_EMCN high
Fetal Kidney Endothelial cell_GJA5 high
17wk fetal nephron forming Proximal tubule
Adult Kidney Proximal tubule cell_ALDOB high
Adult Kidney Intercalated cell_CALB1 high
Adult Kidney Intercalated cell_SPINK1 high
17wk fetal nephron forming Loop of Henle
Adult Kidney Distal convoluted tubule
Fetal kidney Collecting Duct
16-17wk fetal kidney Interstitial Cell Lineages (COL8A1+)
17wk fetal nephron forming Medial-Distal
16wk fetal kidney Differentiating nephron cell-types (MAL+)
16-17wk fetal kidney Differentiated NPC (Distal Precursor)
17wk fetal nephron forming Broad proximal diff
17wk fetal nephron forming Podocyte
Fetal Kidney Podocyte (PMID32214235 top 100)
16-17wk fetal kidney Interstitial Cell Lineages (Cortical Stroma)
Adult Lung Adventitial Fibroblast
Fetal Male Gonad Fibroblast
16wk fetal kidney Interstitial cell lineages (REN+)
Adult Kidney Smooth muscle cell
Pediatric Intestine Fibroblast-TACI
Adult Kidney Epithelial_cell_NUPR1 high
16-17wk fetal kidney Nephron Progenitors (NPC CRABP2+)
16wk fetal kidney cortex Self-Renewing NPCs
17wk fetal nephron forming NPCs
16-17wk fetal kidney Stroma M-phase
16-17wk fetal kidney Stroma G2-M phase
Fetal kidney Cap mesenchyme
16wk fetal kidney Nephron Progenitors
Kidney B cell
Adult Intestine Immune-T.Tcells
16-17wk fetal kidney Monocyte
Adult Kidney Macrophage_APOC1 high
Fetal kidney Monocyte
Adult Intestine Immune-DC2
Pediatric Intestine pDC
Adult Brain Excitatory neuron_CBLN2 high
Z-score
-10
10

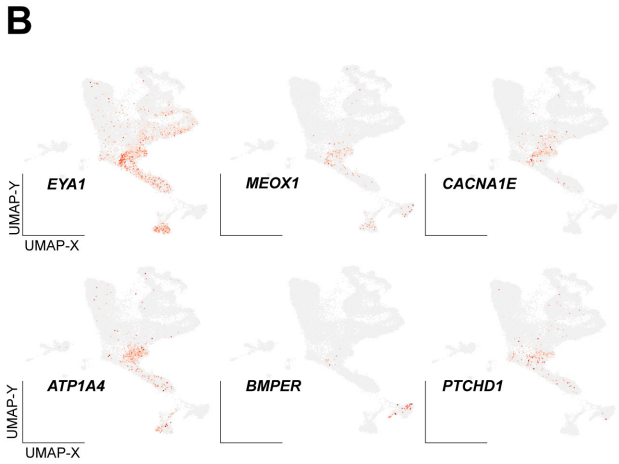
B
EYA1
MEOX1
CACNA1E
ATP1A4
BMPER
PTCHD1
UMAP-Y
UMAP-X

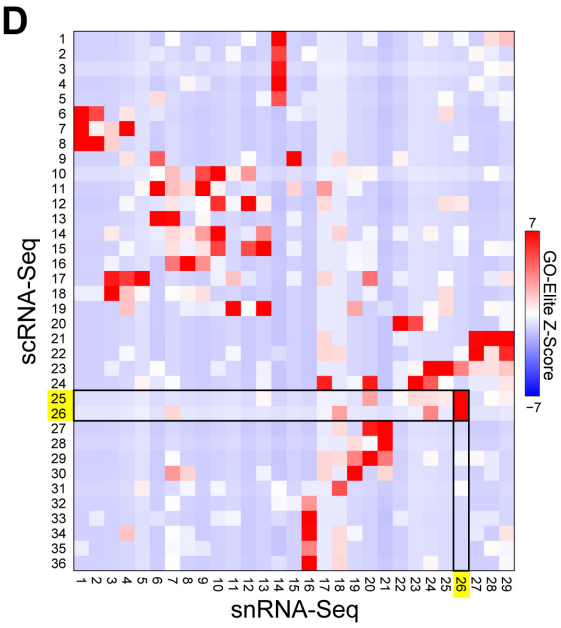
D
scRNA-Seq
snRNA-Seq
GO-Elite Z-Score
7
-7

Figure S4

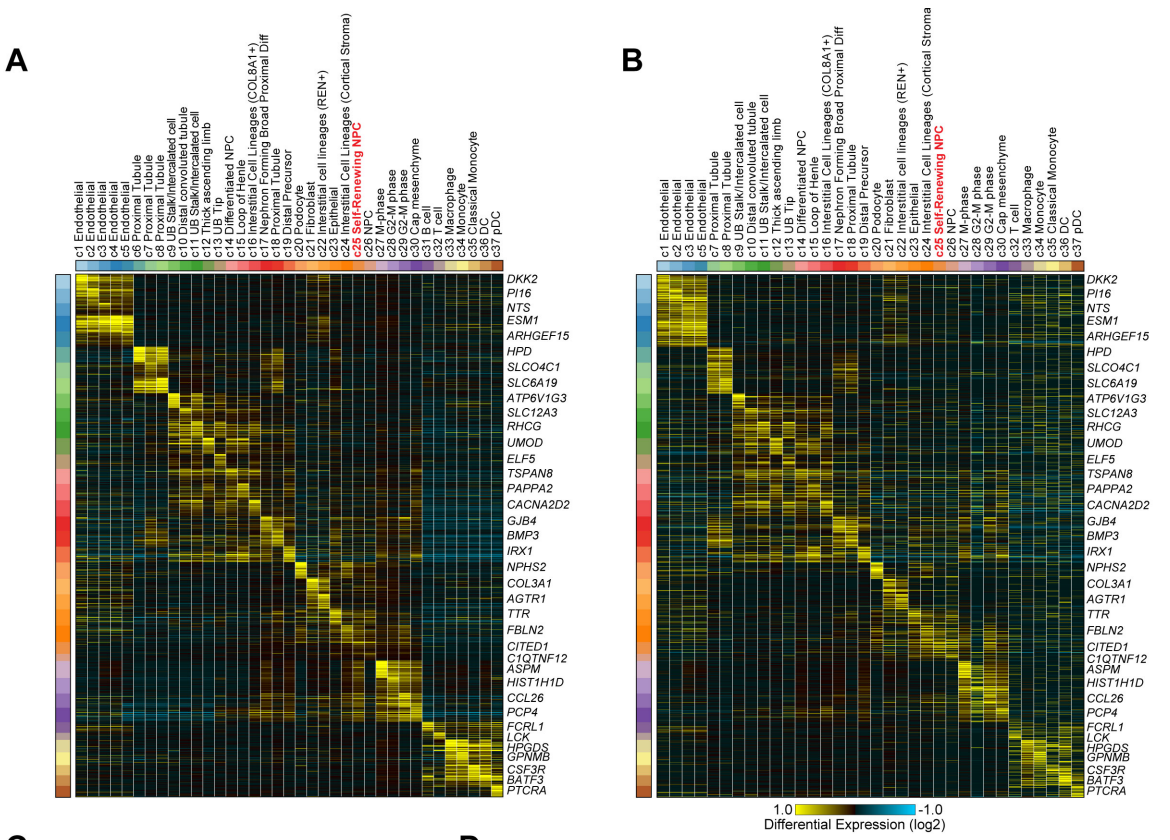
A
B
c1 Endothelial
c2 Endothelial
c3 Endothelial
c4 Endothelial
c5 Endothelial
c6 Proximal Tubule
c7 Proximal Tubule
c8 Proximal Tubule
c9 UB Stalk/Intercalated cell
c10 Distal convoluted tubule
c11 UB Stalk/Intercalated cell
c12 Thick ascending limb
c13 UB Tip
c14 Differentiated NPC
c15 Loop of Henle
c16 Interstitial Cell Lineages (COL8A1+)
c17 Nephron Forming Broad Proximal Diff
c18 Proximal Tubule
c19 Distal Precursor
c20 Podocyte
c21 Fibroblast
c22 Interstitial cell lineages (REN+)
c23 Epithelial
c24 Interstitial Cell Lineages (Cortical Stroma)
c25 Self-Renewing NPC
c26 NPC
c27 M-phase
c28 G2-M phase
c29 G2-M phase
c30 Cap mesenchyme
c31 B cell
c32 T cell
c33 Macrophage
c34 Monocyte
c35 Classical Monocyte
c36 DC
c37 pDC
DKK2
PI16
NTS
ESM1
ARHGEF15
HPD
SLCO4C1
SLC6A19
ATP6V1G3
SLC12A3
RHCG
UMOD
ELF5
TSPAN8
PAPPA2
CACNA2D2
GJB4
BMP3
IRX1
NPHS2
COL3A1
AGTR1
TTR
FBLN2
CITED1
C1QTNF12
ASPM
HIST1H1D
CCL26
PCP4
FCRL1
LCK
HPGDS
GPNMB
CSF3R
BATF3
PTCRA
1.0
-1.0
Differential Expression (log2)

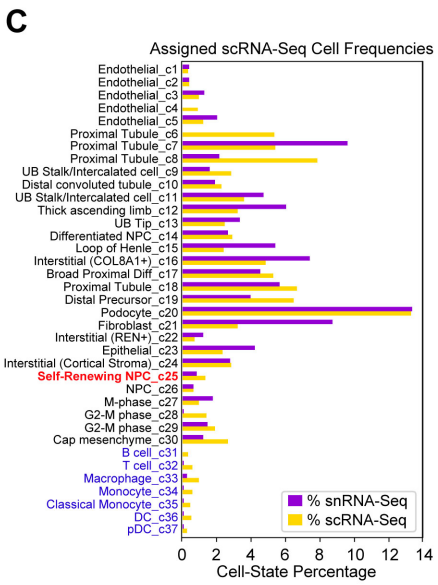
C
Assigned scRNA-Seq Cell Frequencies
Endothelial_c1
Endothelial_c2
Endothelial_c3
Endothelial_c4
Endothelial_c5
Proximal Tubule_c6
Proximal Tubule_c7
Proximal Tubule_c8
UB Stalk/Intercalated cell_c9
Distal convoluted tubule_c10
UB Stalk/Intercalated cell_c11
Thick ascending limb_c12
UB Tip_c13
Differentiated NPC_c14
Loop of Henle_c15
Interstitial (COL8A1+)_c16
Broad Proximal Diff_c17
Proximal Tubule_c18
Distal Precursor_c19
Podocyte_c20
Fibroblast_c21
Interstitial (REN+)_c22
Epithelial_c23
Interstitial (Cortical Stroma)_c24
Self-Renewing NPC_c25
NPC_c26
M-phase_c27
G2-M phase_c28
G2-M phase_c29
Cap mesenchyme_c30
B cell_c31
T cell_c32
Macrophage_c33
Monocyte_c34
Classical Monocyte_c35
DC_c36
pDC_c37
% snRNA-Seq
% scRNA-Seq
0
2
4
6
8
10
12
14
Cell-State Percentage

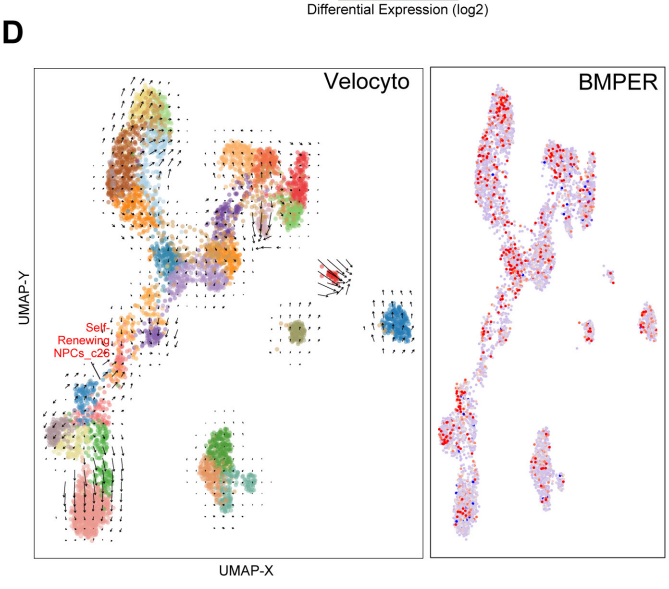
D
Velocyto
BMPER
Self-Renewing NPCs_c25
UMAP-Y
UMAP-X

Figure S5

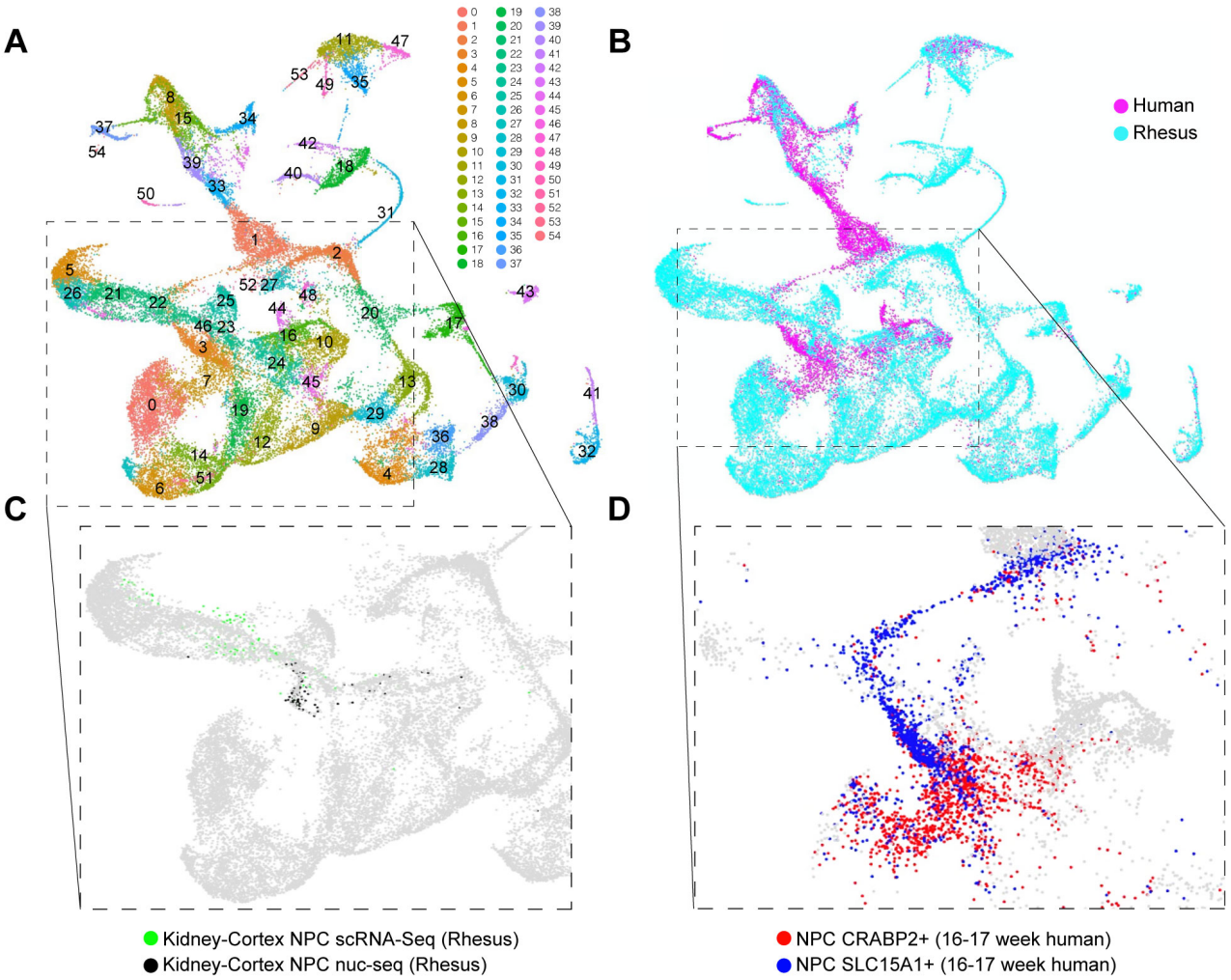
A
B
C
D
Human
Rhesus
Kidney-Cortex NPC scRNA-Seq (Rhesus)
Kidney-Cortex NPC nuc-seq (Rhesus)
NPC CRABP2+ (16-17 week human)
NPC SLC15A1+ (16-17 week human)

Figure S6

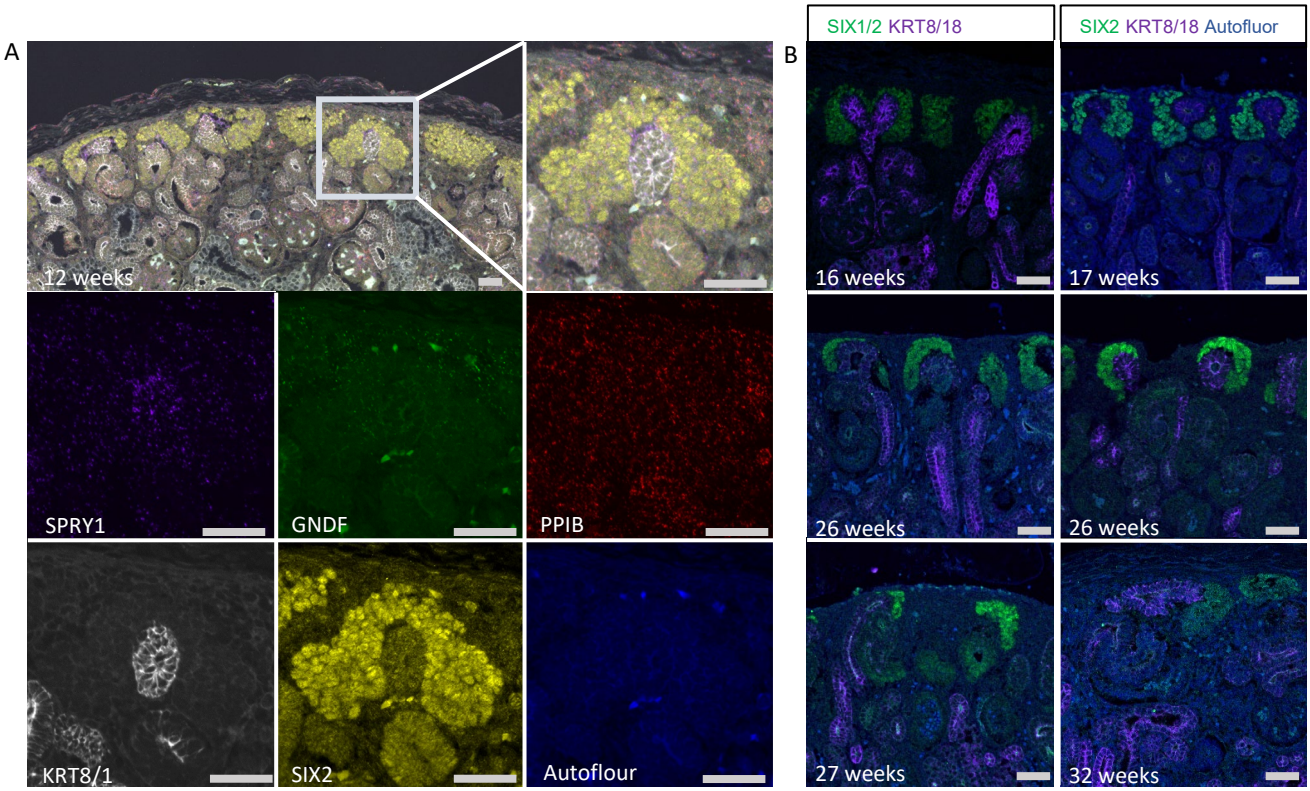
A
12 weeks
SPRY1
GNDF
PPIB
KRT8/1
SIX2
Autoflour
B
SIX1/2 KRT8/18
SIX2 KRT8/18 Autofluor
16 weeks
17 weeks
26 weeks
26 weeks
27 weeks
32 weeks

Figure S7

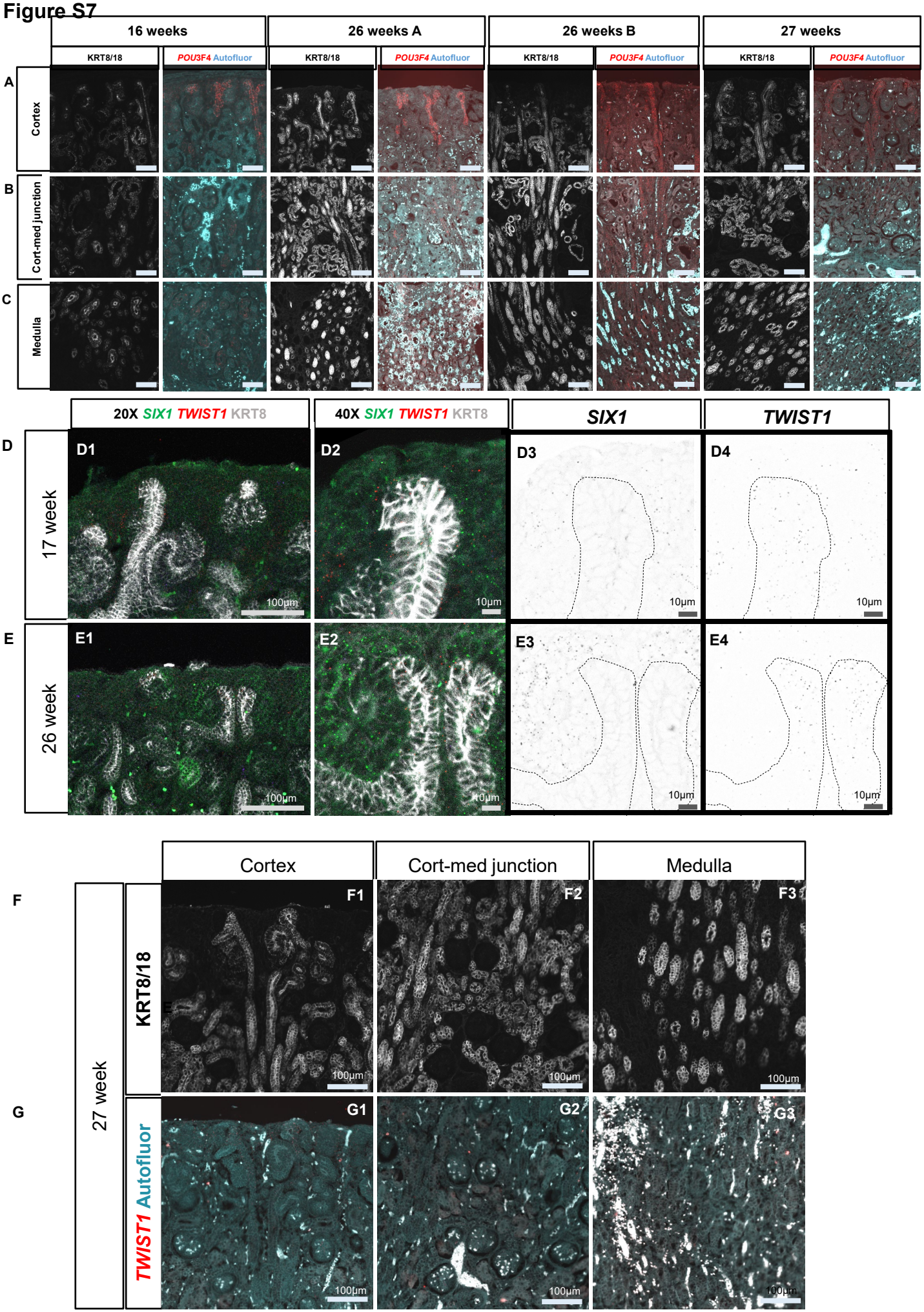
16 weeks
26 weeks A
26 weeks B
27 weeks
KRT8/18
POU3F4 Autofluor
A
Cortex
B
Cort-med junction
C
Medulla
20X SIX1 TWIST1 KRT8
40X SIX1 TWIST1 KRT8
SIX1
TWIST1
D
17 week
D1
D2
D3
D4
E
26 week
E1
E2
E3
E4
100μm
10μm
Cortex
Cort-med junction
Medulla
F
27 week
KRT8/18
F1
F2
F3
G
TWIST1 Autofluor
G1
G2
G3

3. Supplemental Figure Legends

Figure S1: Schematic of Human Nephrogenesis. This figure, adapted from Cullen-McEwen[1], represents human kidney development throughout nephrogenesis. LBN proceeds after arcading, and shows nephrons directly attached to the ureteric stalk

Figure S2: Undifferentiated NPCs are noted in both rhesus and human samples analyzed in this study. A-B: Rhesus samples utilized for scRNAseq were immunostained for SIX1 (green), KRT8/18 (purple) and CDH1 (Panel A) or LAMβ1 (Panel B). Yellow arrows identify NPC populations without lamβ1 staining signifying NPC populations that have not yet epithelialized. Far right panel example of 32-WG human kidney which appears morphologically similar to rhesus samples analyzed in study. C-E: Human archival samples used in RNAScope were stained for CDH1 (C) LAMβ1 (D), and ZO-1 (E) to identify if NPC3 populations had already differentiated. Areas of luminalization are identified with white arrow, while examples without luminalization are identified by yellow asterisk. Scale bar = 100 microns.

Figure S3: Annotation and alignment of scRNA-Seq and snRNA-Seq clusters. A,C) Top enriched human cell-type gene-sets from the software GO-Elite, applied to ICGS2 scRNA-Seq (A) and snRNA-Seq clusters (C) (top 100 marker genes/cluster analyzed). B) Visualization of z-score normalized gene-expression levels, for example NPC marker genes. Cluster 25 cells are denoted with a dashed line. D) Enrichment of snRNA-Seq cluster relative to scRNA-Seq obtained clusters.

Figure S4: Common kidney progenitor populations in cortex single cells and nuclei. A,B) Common marker genes identified in cortex scRNA-Seq (A) and single-cell cellHarmony aligned snRNA-Seq (B). The top marker gene per cluster is displayed on the right of each cluster. C) Cell populations frequencies of scRNA-Seq and aligned snRNA-Seq. D) Overlayed RNA

velocity predictions snRNA-Seq cell populations (left) and gene relative velocities for nuclei with expression of the NPC marker gene BMPER.

Figure S5: Maturation associated differences in nephron progenitors across species. A) A-D) Integrated analysis of 3 human and 5 rhesus kidney scRNA-Seq/snRNA-Seq datasets using the software Seurat3. All 54 predicted cell clusters are displayed (A), along with either rhesus or human (B) cells and progenitor clusters called out for each species (C,D) based on ICGS2 defined cell-clusters (see Figure 3 and Methods). E) Prediction of cell-type identity for all Seurat3 clusters based on GO-Elite analysis compared to the human compendium single-cell RNA-Seq BioMarker database in AltAnalyze.

Figure: S6 Previous work supporting RNA and protein stability in human archival material. A) 12-week human kidney with PMI 72 hours with RNAScope probes for *SPROUTY*1(*SPRY 1*, detects UB tip), *GDNF* (detects NPC), *PPIB* (RNAScope recommended positive control), antibodies to KRT8/18 (UB), SIX2 (NPC), and channel for autofluorescence. B) Human archival samples used for validation studies with corresponding gestational ages. Immunofluroescence confirms presence of SIX2 NPCs. Autofluorescence = autofluor. Scale bar = 50μm.

Figure S7: RNAScope validation of UB markers *POU3F4* and *TWIST1*. A-C) Widefield images of antibody stain and RNAScope in situ hybridization. Images were obtained at 20x objective on the widefield microscope to determine presence or absence of *POU3F4* (red) in the cortex, cortical medullary junction, and medulla in 16 WG, two 26 WG, and 27 WG human archival samples. Non-specific autofluorescent signal in light blue. Red signal is detected both in the cortical medullary junction (cort-med junction (B) and medulla (C) but most prominently in the cortex (A). D-E) Confocal images of antibody stain and RNAScope in situ hybridization. RNA

probes for *SIX1* (green) and *TWIST1*(red) as well as antibodies to KRT8/18 (collecting duct) were used to localize the transcripts in human archival material at 17 (D) and 26 (E) WG. KRT8/18 staining outlined in D3-4, E3-4. *TWIST1* co-localized krt8/18 ureteric tip at both gestational ages (D4, E4), but also appeared out of the region identified by the KRT8 signal or *SIX1* (D3, E3). F-G) Widefield images of antibody stain and RNAScope in situ hybridization. Images were obtained at 20x objective on the widefield microscope to determine presence or absence of *TWIST1*(red) in the cortex, cortical medullary junction, and medulla of human archival samples. This figure represents an example at 27 WG. Non-specific autofluorescent signal in light blue. RNA transcript signal can be seen in the peripheral cortex, both in UB and stroma (G1), but no specific signal is identified in cortical-medullary junction (G2) or medulla (G3).

References:

1. Cullen-McEwen LS, M.; Black, MJ.: Kidney Development, Disease, Repair and Regeneration. p. 27-37., 2016

4. **Supplemental Spread sheet: Supplemental Tables** (see excel spreadsheet)
5. **Supplemental Spread sheet: Supplemental data 1 Rhesus morphology** (see excel spreadsheet)
6. **Supplemental Spread sheet: Supplemental data 2 RNAScope** (see excel spreadsheet)
7. **Supplemental Movies 1 and 2**
    a. Supplemental Movie 1: 32 WG human kidney; example of ureteric stalk displaying lateral branch nephrogenesis. SIX2 (green), CDH1 (red), KRT (purple).
    b. Supplemental Movie 2: 129 DG rhesus kidney; example of ureteric stalk displaying lateral branch nephrogenesis. SIX2 (green), CDH1 (red), KRT (purple).